Piecewise polynomial electronic wavefunctions

José Luis Gázquez*† and Harris J. Silverstone

Department of Chemistry, The Johns Hopkins University, Baltimore, Maryland 21218
(Received 23 July 1976)

Piecewise polynomials are examined as basis functions for electronic wavefunctions. The spline function method is a special case, which is shown to be less accurate, for a fixed set of mesh points, than a method based directly on Hermite's interpolation formula. The determination of a suitable mesh is discussed both inductively and deductively, and a logarithmic formula for the $1s$ orbital of helium is "derived." The accuracy is shown to depend on the number of points $N+1$ and on the polynomial order $2s+1$, approximately according to the formula, $\delta E \sim N^{-4s-2}$, for appropriate meshes. A striking result is the possibility for systematically increasing the accuracy of the energy by systematically increasing the number of points, without encountering linear dependence problems, is demonstrated by calculations on the helium atom. With a 16-point theoretically derived mesh, and with seventh order polynomials, we obtain a Hartree–Fock energy for helium of -2.8616799956122 a.u.

I. INTRODUCTION

Perhaps because they are so simple, polynomials have been largely neglected as basis functions for electronic wavefunctions. In the last few years, Shore,[1–3] Gilbert and Bertoncini,[4] and Altenberger-Siczek and Gilbert[5] have discussed a special class of piecewise polynomial functions called splines, with quantum mechanical calculations on the hydrogen atom, the Morse oscillator, and the helium atom. Shore showed that a large number of bound and scattering states for hydrogen and other one dimensional problems could be accurately reproduced by splines, and that higher order septic and quintic splines were more efficient than cubic splines. On the other hand, Altenberger-Siczek and Gilbert, who treated helium with cubic splines, were rather pessimistic about the suitability of splines for self-consistent field calculations. In this paper we discuss, along with splines, more general piecewise polynomial representations. We shall demonstrate that piecewise polynomials are capable of several orders of magnitude more accuracy than splines. Indeed, the accuracy of the helium atom Hartree–Fock energy with a 14-point seventh order piecewise polynomial representation is 1.5×10^{-13} a.u., which is 7.7 orders of magnitude smaller than the 8.9×10^{-6} a.u. error reported by Altenberger-Siczek and Gilbert[5] with a 16-point cubic spline function!

A particular piecewise polynomial representation is characterized by the *order* of the polynomials, the *mesh points* at which the representation changes from one polynomial to the next, and the *connection formulas* that connect the polynomials on the different intervals. By *connection formula* we mean the relationships the coefficients of polynomials on adjacent intervals must satisfy, for a specified number of derivatives to be continuous at the common end point. These are discussed via the Hermite interpolation formula in Sec. III. In Sec. IV the influence of *order* and *mesh* on accuracy is discussed, and, for example, the error in the Hartree–Fock energy of helium is predicted to depend on the number of points $N+1$ and the polynomial order $2s+1$ according to

$$\delta E \sim N^{-4s-2} . \tag{1}$$

Piecewise polynomials are a hybrid of numerical and analytical representations of wavefunctions. We emphasize at the start, however, that they are used here strictly in a variational context characteristic of the usual analytical representations of wavefunctions. Some features of numerical approaches do remain, nevertheless, such as the possibility for *systematically* increasing the accuracy by *systematically* increasing the fineness of the mesh. The systematization particularly contrasts this method with the more usual analytical expansion methods, in which a systematic method for choosing orbital exponents is usually lacking (the notable exception being the "even-tempered atomic orbital" approach—cf. Raffenetti[6]). Moreover, some features of the usual variational approaches seem to be absent, such as the linear dependence problem that plagues large Slater orbital or Gaussian orbital bases.

Our purpose in this paper is to outline the main features of piecewise polynomial electronic wavefunctions, and to illustrate their capacity for systematically high accuracy by Hartree–Fock calculations on the helium atom.

II. PIECEWISE POLYNOMIAL VS POLYNOMIAL REPRESENTATIONS

In principle an electronic radial wavefunction can be approximated by a single polynomial. The boundary condition at infinity of square integrability can be approximated by having the polynomial vanish at a large value of r, say r_N. Then on the interval $[0, r_N]$ the approximation can be made arbitrarily accurate by taking the order of the polynomial sufficiently high.

In practice, the result is analogous to a truncated power series for $\exp(-r)$ for large r. Even though the mathematical convergence is absolute, the cancellation of exponentially large positive and negative contributions to an exponentially small sum renders the polynomial computationally useless.

The piecewise polynomial approach avoids this exponential catastrophe by subdividing the interval $[0, r_N]$ by points $r_1 < r_2 < \cdots < r_{N-1}$. On each subinterval $[r_{n-1}, r_n]$ a different polynomial is used that need accurately represent the function only on that subinterval. Since the expansion variable is effectively $(r - r_{n-1})$ rather than r

in $(r - r_{n-1})$ will be computationally useful.

We shall elaborate on two piecewise polynomial schemes in detail: the spline function method, and the "Hermite interpolation function" method that will be defined below.

III. CONTINUITY AND CONNECTION FORMULAS

Different piecewise polynomial representations may be distinguished by the highest derivative that remains continuous at the mesh points $r_1, r_2, \ldots, r_{N-1}$. Since the Hermite interpolation formula[7] expresses a polynomial in terms of its values and derivatives at a number of points, it is ideally suited for discussing continuity at end points. The Hermite interpolation polynomial that takes on the values $y_{n-1}^{(0)}$ at r_{n-1} and $y_n^{(0)}$ at r_n, and whose derivatives are $y_{n-1}^{(i)}$ and $y_n^{(i)}$, $i = 1, 2, \ldots, s$ at the respective end points, is of $2s+1$th order. For $s = 1$, 2, and 3, the formulas are stated below:

$$p_{3,[n-1,n]}(r) = y_{n-1}^{(0)}\frac{r_n - r}{r_n - r_{n-1}} + y_n^{(0)}\frac{r - r_{n-1}}{r_n - r_{n-1}} + [(r_n - r_{n-1})y_{n-1}^{(1)} - (y_n^{(0)} - y_{n-1}^{(0)})]\frac{(r - r_{n-1})(r_n - r)^2}{(r_n - r_{n-1})^3}$$

$$- [(r_n - r_{n-1})y_n^{(1)} - (y_n^{(0)} - y_{n-1}^{(0)})]\frac{(r - r_{n-1})^2(r_n - r)}{(r_n - r_{n-1})^3}, \tag{2}$$

$$p_{5,[n-1,n]}(r) = p_{3,[n-1,n]}(r) + \frac{1}{2!}[(r_n - r_{n-1})^2 y_{n-1}^{(2)} + (r_n - r_{n-1})(4y_{n-1}^{(1)} + 2y_n^{(1)}) - 6(y_n^{(0)} - y_{n-1}^{(0)})]\frac{(r - r_{n-1})^2(r_n - r)^3}{(r_n - r_{n-1})^5}$$

$$+ \frac{1}{2!}[(r_n - r_{n-1})^2 y_n^{(2)} - (r_n - r_{n-1})(2y_{n-1}^{(1)} + 4y_n^{(1)}) + 6(y_n^{(0)} - y_{n-1}^{(0)})]\frac{(r - r_{n-1})^3(r_n - r)^2}{(r_n - r_{n-1})^5}, \tag{3}$$

$$p_{7,[n-1,n]}(r) = p_{5,[n-1,n]}(r) + \frac{1}{3!}[(r_n - r_{n-1})^3 y_{n-1}^{(3)} + (r_n - r_{n-1})^2(9y_{n-1}^{(2)} - 3y_n^{(2)}) + (r_n - r_{n-1})(36y_{n-1}^{(1)} + 24y_n^{(1)})$$

$$- 60(y_n^{(0)} - y_{n-1}^{(0)})]\frac{(r - r_{n-1})^3(r_n - r)^4}{(r_n - r_{n-1})^7} - \frac{1}{3!}[(r_n - r_{n-1})^3 y_n^{(3)} + (r_n - r_{n-1})^2(3y_{n-1}^{(2)} - 9y_n^{(2)})$$

$$+ (r_n - r_{n-1})(24y_{n-1}^{(1)} + 36y_n^{(1)}) - 60(y_n^{(0)} - y_{n-1}^{(0)})]\frac{(r - r_{n-1})^4(r_n - r)^3}{(r_n - r_{n-1})^7}. \tag{4}$$

itself, for a sufficiently fine subdivision the polynomial

The Hermite interpolation formula suggests a particular piecewise polynomial scheme, which we call the *Hermite interpolation function* (HIF) scheme. It is defined by: (1) The polynomial order is $2s+1$; (2) The function and its first s derivatives are to be continuous at the interior mesh points $r_1, r_2, \ldots, r_{n-1}$. Operationally, the $(s+1)\times(N+1)$ quantities $y_n^{(i)}$, $(i = 0, 1, \ldots, s)$, $(n = 0, 1, \ldots, N)$, are the independent linear parameters in the variational energy calculation. The Hermite interpolation formula gives each of the N polynomials $p_{2s+1,[n-1,n]}(r)$, which involve a total of $N\times(2s+2)$ polynomial coefficients, in terms of the $y_n^{(i)}$ in such a way as to make the polynomials $p_{2s+1,[n-1,n]}(r)$ and $p_{2s+1,[n,n+1]}(r)$ automatically match their values and first s derivatives at $r = r_n$.

The *spline function* scheme[8] goes further than the HIF scheme in its continuity requirements and eventually makes the derivatives $y_n^{(i)}$, $(i \geq 1)$, linearly dependent on the functional values $y_n^{(0)}$, thus drastically reducing the number of linearly independent variational parameters to $N+1$. The *spline* scheme is defined by: (1) The polynomial order is $2s+1$; (2) The function and all its derivatives through order $2s$ are to be continuous at the interior mesh points $r_1, r_2, \ldots, r_{N-1}$. One cannot require the $2s+1$st derivatives to be continuous, because the solution would then be a single polynomial of order $2s+1$ on $[0, r_N]$. To incorporate the continuity of the $s+1$st through $2s$th derivatives, one sets equal the appropriate derivatives of $p_{2s+1,[n-1,n]}(r)$ and $p_{2s+1,[n,n+1]}(r)$ at their common end point:

$$(d/dr)^i p_{2s+1,[n-1,n]}(r)\big|_{r=r_n} = (d/dr)^i p_{2s+1,[n,n+1]}(r)\big|_{r=r_n},$$

$$(i = s+1, s+2, \ldots, 2s;\ n = 1, 2, \ldots, N-1). \tag{5}$$

If the $s\times(N-1)$ simultaneous linear equations so obtained are supplemented by $2s$ homogeneous linear boundary conditions, then the resulting $s\times(N+1)$ simultaneous linear equations can be solved to express the derivatives in terms of the functional values:

$$y_n^{(i)} = \sum_{n'=0}^{N} Z_{nn'}^{(i)} y_{n'}^{(0)}, \quad (i = 1, 2, \ldots, s). \tag{6}$$

The $Z_{nn'}^{(i)}$ depend only on the mesh points $(0, r_1, r_2, \ldots, r_N)$ and on the boundary conditions, but not on the function being approximated. The details are given in Appendix A. Operationally we may characterize the spline function method as follows: (1) The $N+1$ quantities $y_n^{(0)}$ are the independent linear variational parameters. (2) The $s\times(N+1)$ quantities $y_n^{(i)}$ are obtained from the $y_n^{(0)}$ via Eqs. (6). (3) The Hermite interpolation formula gives each of the N polynomials $p_{2s+1,[n-1,n]}(r)$ in such a way as to make the polynomials $p_{2s+1,[n-1,n]}(r)$ and $p_{2s+1,[n,n+1]}(r)$ automatically match their values and first s derivatives at $r = r_n$. (4) The Eqs. (6) further guarantee that the $s+1$th through $2s$th derivatives will be continuous.

One can envisage intermediate schemes for which the polynomial order would be $2s+1$, but the highest order derivative required to be continuous would be neither s nor $2s$. The discussion would proceed along one of the above lines. We have not treated such schemes in our computations.

TABLE I. Mesh points for cubic polynomials, obtained by the "window" method.

ϵ[a]	10^{-4}	10^{-5}	10^{-6}	10^{-7}	10^{-8}	10^{-9}
N	7	10	14	21	29	39
Points[b]	0.00	0.00	0.00	0.00	0.00	0.00[c]
	0.45	0.30	0.25	0.20	0.15	0.05
	0.95	0.65	0.50	0.35	0.25	0.15
	1.60	1.00	0.75	0.50	0.35	0.20
	2.50	1.45	1.00	0.65	0.45	0.25
	3.85	2.00	1.30	0.85	0.55	0.30
	6.25	2.75	1.60	1.05	0.65	0.35
	14.50	3.75	2.05	1.20	0.75	0.45
		5.30	2.50	1.35	0.90	0.55
		8.45	3.10	1.50	1.05	0.65
		>25.00	3.85	1.65	1.20	0.75
			4.90	1.95	1.35	0.82
			6.65	2.25	1.50	0.90
			10.65	2.55	1.65	0.98
			>25.00	3.00	1.80	1.05
				3.45	1.95	1.13
				4.05	2.10	1.20
				4.80	2.25	1.35
				5.90	2.40	1.50
				7.75	2.70	1.65
				12.00	3.00	1.80
				>25.00	3.30	1.95
					3.60	2.10
					4.05	2.25
					4.50	2.40
					5.10	2.55
					5.85	2.70
					7.10	2.85
					9.35	3.00
					15.85	3.15
						3.30
						3.60
						4.05
						4.50
						5.10
						5.85
						6.85
						7.85
						8.85
						10.00

[a]Energy error contributed by each subinterval, in atomic units (27.2...eV).
[b]In atomic units (Bohr radii).
[c]This set of points was extrapolated with the aid of Fig. 1. It was not calculated directly by the "window" method.

IV. CHOICE OF MESH

A. The window method

The choice of mesh points is crucial to the efficiency of piecewise methods. Since the mesh points enter as nonlinear parameters, their variational optimization would be difficult. Both Shore[1-3] and Gilbert and Bertoncini[4] have used various formulas, but the theoretical basis for their formulas seems obscure. We first exploit an inductive approach, the "window" method, to discern whether there are any "natural rules" for choosing mesh points.

Suppose one has a radial Hamiltonian and its exact wavefunction $R(r)$. To be determined is a mesh with the property that, when $R(r)$ is replaced by a piecewise polynomial approximating function, each subinterval contributes equally to the error in the expectation value for the energy. Begin by cutting a "window" in $R(r)$ from 0 to r_1. For $0 \le r \le r_1$, replace $R(r)$ by the Hermite interpolation polynomial, with the requisite functional and derivative values taken from $R(r)$. For $r \ge r_1$, $R(r)$ remains unchanged. Calculate the energy with this composite wavefunction as a function of r_1, and find the value of r_1 at which the energy has increased by a predetermined amount ϵ over its exact value. Fix this value of r_1 as one of the mesh points. Next cut a "window" in $R(r)$ from r_1 (fixed above) to r_2. For $0 \le r \le r_1$, and $r \ge r_2$, keep $R(r)$ unchanged, but for $r_1 \le r \le r_2$, replace $R(r)$ by a Hermite interpolation polynomial. Calculate the energy as a function of r_2 to find the value at which the energy is ϵ greater than its exact value. This determines the mesh point r_2, and so forth for $r_3, r_4, \ldots$. In such a manner, an "energy equal error" mesh can be defined.

TABLE II. Mesh points for quintic polynomials, obtained by the "window" method.

ϵ[a]	10^{-4}	10^{-5}	10^{-6}	10^{-7}	10^{-8}	10^{-9}
N	4	5	6	8	9	12
Points[b]	0.00	0.00	0.00	0.00	0.00	0.00
	1.15	1.00	0.85	0.75	0.65	0.40
	2.70	2.15	1.70	1.35	1.10	0.80
	5.50	4.00	2.90	2.20	1.65	1.20
	12.00	7.30	4.70	3.30	2.35	1.65
		16.50	7.80	4.90	3.20	2.20
			16.00	7.40	4.45	2.85
				12.50	6.15	3.70
				>25.00	8.75	4.70
					15.00	6.10
						8.00
						11.50
						>15.00

[a]Energy error contributed by each subinterval, in atomic units (27.2...eV).
[b]In atomic units (Bohr radii).

We have applied the "window" method to the Hartree–Fock 1s radial orbital for helium, where Raffenetti's even-tempered Slater orbital representation[6] has been used for the exact $R(r)$. The "window points" for various values of ϵ for cubic, quintic, and septic polynomials, are listed in Tables I–III.

To bring out possible regularities in the "window points" the logarithms of the differences, $\log(r_n - r_{n-1})$, have been plotted vs r_{n-1} in Figs. 1–3. Examinations of Figs. 1–3 shows that in each case, cubics, quintics,

TABLE III. Mesh points for septic polynomials, obtained by the "window" method.

ϵ[a]	10^{-4}	10^{-5}	10^{-6}	10^{-7}	10^{-8}
N	4	4	4	5	6
Points[b]	0.00	0.00	0.00	0.00	0.00
	1.50	1.20	1.00	0.80	0.65
	4.25	3.20	2.50	1.95	1.625
	10.50	7.10	5.20	3.80	3.00
	>25.00	14.40	10.40	6.70	4.925
				12.70	8.30
					14.40

[a]Energy error contributed by each subinterval, in atomic units (27.2...eV).
[b]In atomic units (Bohr radii).

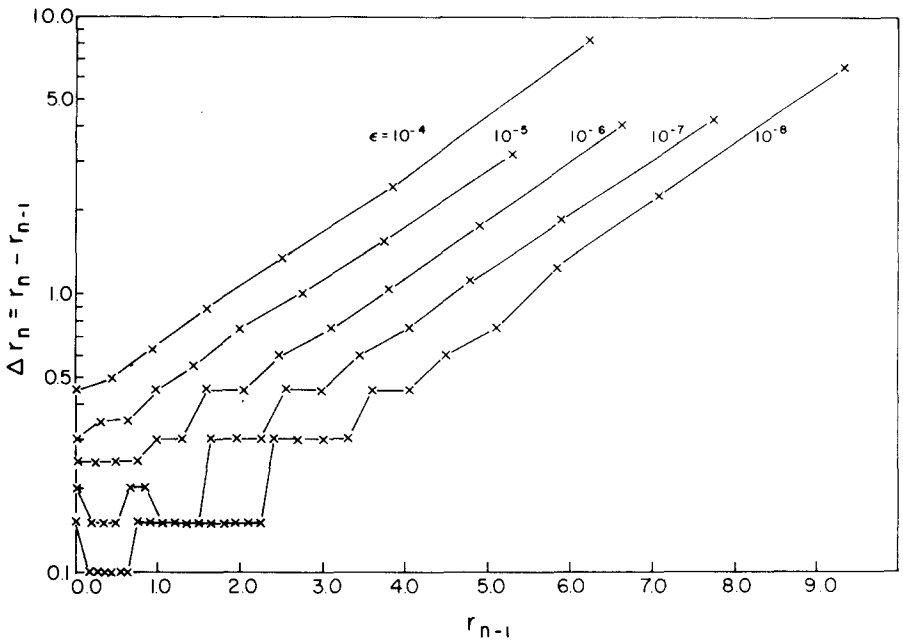

FIG. 1. "Window" mesh points for cubic polynomials for helium 1s orbital. Plot of $\Delta r_n = r_n - r_{n-1}$ (logarithmic scale) vs r_{n-1}.

and septics, the $\log\Delta r$ vs r curves are approximately parallel, approximately equally spaced, and for large r are approximately straight lines. This striking behavior is examined *a priori* in the next subsection.

B. Theory

The empirical rule satisfied by the "window points" can be cast in a form with a more general significance, one that also makes sense intuitively. Notice that $\log\Delta r$ can be written $-\log(\Delta n/\Delta r)$, since $\Delta n = 1$. Replace the discrete "density of points" function $\Delta n/\Delta r$ by an idealized continuous density of points function dn/dr. That the $\log\Delta r$ curves are parallel and equally spaced implies that dn/dr satisfies the equation,

$$dn/dr = f_{2s+1}(r)\epsilon^{-k_{2s+1}} . \tag{7}$$

Here $f_{2s+1}(r)$ is a function of r and the polynomial order $2s+1$, but not of the accuracy parameter ϵ or of n. The k_{2s+1} is a constant with respect to r, ϵ, and n; it does depend on the polynomial order. Thus the density of points is given by the product of a scale factor that depends on the accuracy and a factor that depends on r.

The basis for Eq. (7) is empirical. Now we derive the same result nonempirically. To obtain a more definitive theory for dn/dr, it is necessary to examine the detailed contribution to the energy error from the subinterval $[r_{n-1}, r_n]$. Assume that $y_{n-1}^{(i)}$ and $y_n^{(i)}$, $(i = 0, 1, 2, \ldots, s)$, have the values taken on by the exact radial wavefunction $R(r)$. The error introduced by the interpolation polynomial between r_{n-1} and r_n is[7]

$$\delta R_n = (r - r_{n-1})^{s+1}(r_n - r)^{s+1} R^{(2s+2)}(\bar{r})/(2s+2)! , \tag{8}$$

where $\bar{r}$ is some mean value of r between r_{n-1} and r_n. The error contributed by δR_n to the total electronic en-

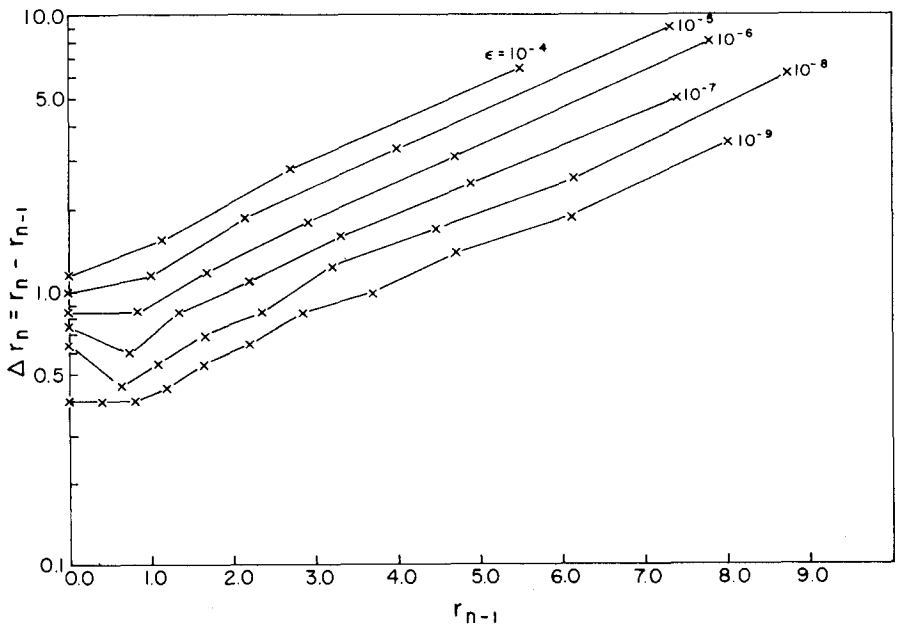

FIG. 2. "Window" mesh points for quintic polynomials for helium 1s orbital. Plot of $\Delta r_n = r_n - r_{n-1}$ (logarithmic scale) vs r_{n-1}.

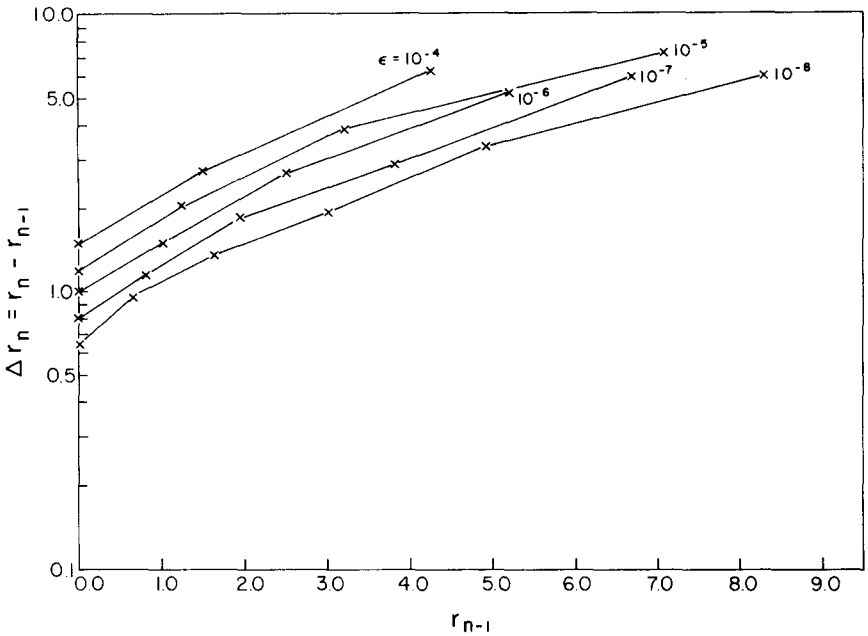

FIG. 3. "Window" mesh points for septic polynomials for helium 1s orbital. Plot of $\Delta r_n = r_n - r_{n-1}$ (logarithmic scale) vs r_{n-1}.

ergy error is (in the usual Dirac notation)

$$\epsilon = \langle \delta R_n | F | \delta R_n \rangle \ , \tag{9}$$

where F is the (radial) Fock operator. For the helium ground state, the kinetic energy term is lowest order in $(r_n - r_{n-1})$ and dominates $\langle \delta R_n | F | \delta R_n \rangle$:

$$\epsilon = \langle \delta R_n | F | \delta R_n \rangle \sim \int_{r_{n-1}}^{r_n} \tfrac{1}{2}[(d/dr) r \delta R_n]^2 \, dr$$

$$= \tfrac{1}{4}(r_n - r_{n-1})^{4s+3}[\bar{r} R^{(2s+2)}(\bar{r})]^2/[(2s+1)(4s+3)!\,] + O[(r_n - r_{n-1})^{4s+4}] \ . \tag{10}$$

(Strictly, the above equation is valid for $r_{n-1} \neq 0$. For $r_{n-1} = 0$, there is a slight change in the numerical factor that is of no consequence to the discussion here.) Set $r_n - r_{n-1} = dr/dn$ and solve for dn/dr:

$$\frac{dn}{dr} = \left\{ \frac{[r R^{(2s+2)}(r)]^2}{4(2s+1)(4s+3)!} \right\}^{1/(4s+3)} \epsilon^{-1/(4s+3)} \ . \tag{11}$$

Thus the $f_{2s+1}(r)$ of Eq. (7) involves the $2s+2$nd derivative of $R(r)$, and the k_{2s+1} is simply $1/(4s+3)$. Equation (11) ought to be of general validity.

A still simpler result can be obtained for the helium example by the (oversimplified) assumption

$$r R^{(2s+2)}(r) \sim \lambda \exp(-\zeta r) \ , \tag{12}$$

where λ and ζ are constants, ζ being related to the 1s orbital energy ϵ_{1s} by

$$\zeta = \sqrt{-2\epsilon_{1s}} \ . \tag{13}$$

Then Eq. (11) becomes

$$\frac{dn}{dr} = \left[\frac{\lambda^2}{4(2s+1)(4s+3)!} \right]^{1/(4s+3)} e^{-2\zeta r/(4s+3)} \epsilon^{-1/(4s+3)} \ . \tag{14}$$

The plot of $\log(dn/dr)$ vs r from Eq. (14) is a straight line! Equation (14) can be solved for r as a function of n:

$$r = -\frac{4s+3}{2\zeta} \log_e(1 - \Lambda \epsilon^{1/(4s+3)} n) \ . \tag{15}$$

Here Λ is a constant arising from the λ-dependent factor in Eq. (14). The integration constant has been chosen so that $n = 0$ corresponds to $r = 0$.

In Figs. 4–6, the logarithmic meshes specified by Eq. (15) are compared with the cubic, quintic and septic "window" meshes. In each case, three successive "window" meshes were selected. A value of $\Lambda \epsilon^{1/(4s+3)}$ was found to make a logarithmic curve approximately match the middle of the three window curves. Then two additional logarithmic curves were obtained by replacing ϵ in Eq. (15) by $\epsilon \times 10^{\pm 1}$. The ζ was fixed by Eq. (13) at 1.35496. The degree of agreement and disagreement (particularly for small values of r) can be judged by the reader.

Equation (15) has almost the same form as Gilbert and Bertocini's "logarithmic mesh,"[4] and the above derivation can be regarded as a partial justification of their formula. However, there is a suble difference in that the constant multiplying the logarithm is fixed $[(4s+3)/2\zeta]$, whereas there it is adjustable. Only for a specific choice of their parameters are the two formulas identical.

Equation (15) also yields a simple prediction of the dependence of accuracy on both the number of points and polynomial order. The maximum value n may take before the argument of the logarithm goes negative is given by

$$N \sim \Lambda^{-1} \epsilon^{-1/(4s+3)} \ . \tag{16}$$

Solving for $N\epsilon$ (each of the N subintervals contributes ϵ to the total error), we obtain

$$\delta E = N\epsilon = \Lambda^{-(4s+3)} N^{-(4s+2)} \ . \tag{17}$$

Since Λ has a complicated dependence on s, it is perhaps more useful to write a simpler expression that omits it:

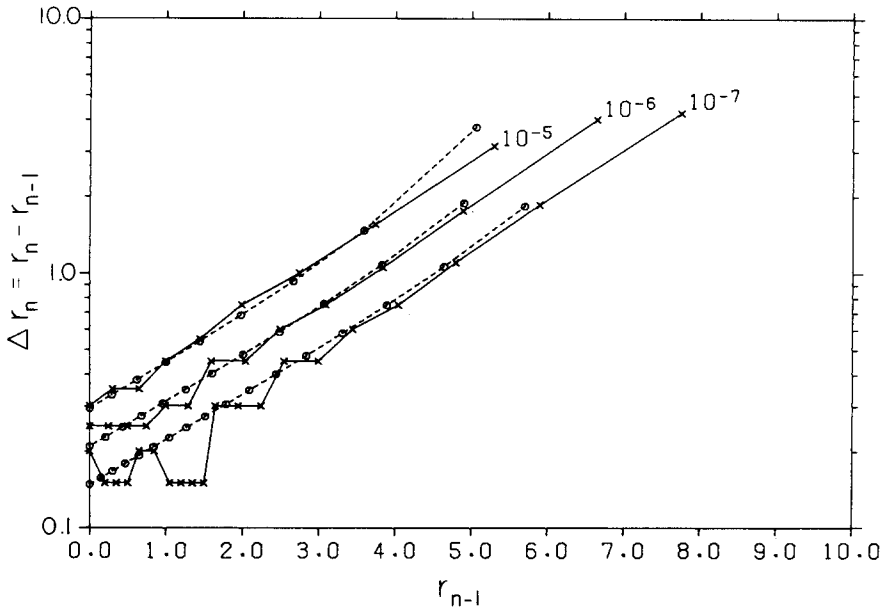

FIG. 4. Cubic "window" mesh points (solid line) for $\epsilon = 10^{-5}$, 10^{-6} and 10^{-7}, and three logarithmic meshes (broken line). The parameters for the logarithmic meshes are: $(4s+3)/2\zeta = 1/0.387$; and $A\epsilon^{1/(4s+3)} = 0.0773\times10^{1/7}$, 0.0773, $0.0773\times10^{-1/7}$. The $A\epsilon^{1/(4s+3)}$ parameter for the middle curve was chosen to place it approximately on the middle "window" curve.

$$\delta E \sim N^{-(4s+2)}, \tag{18}$$

where the polynomial order is $2s+1$.

The inference one draws is that if the mesh is chosen according to Eq. (15), the Hartree–Fock energy will be approached at a rate given by Eq. (18). The convergence rate for cubics is predicted to be N^{-6} (as noticed computationally by Altenberger-Siczek and Gilbert[5]), for quintics N^{-10}, and for septics N^{-14}. The convergence advantages of higher order polynomials are manifestly obvious.

C. Remarks

It is to be emphasized that the basic theoretical equation for the point density is Eq. (11), not the logarithmic formula (15). The logarithmic formula follows from the approximation of the $1s$ orbital in helium by a single exponential [Eq. (12)]. That approximation, while apparently not bad for a $1s$ orbital, would not be expected to be as appropriate for other orbitals, such as $2s$, $2p$, etc.

In the derivation of Eq. (11), the wavefunction and its first s derivatives were assumed to take on their exact values at the mesh points, but in practice, we obtain these values variationally. The variational error will be smaller, but the discrepancy is probably not of great consequence. The exception is that the variational flexibility permits the "kinetic energy error" and "potential energy error," computed with the variational wavefunctions, to tend to equalize, rather than be dominated by the kinetic energy.

Also in the derivation of Eq. (11), the n was taken as a continuous, indeed differentiable, variable. One measure of the inappropriateness of this assumption is the change in the difference quotient $\Delta n/\Delta r$, between

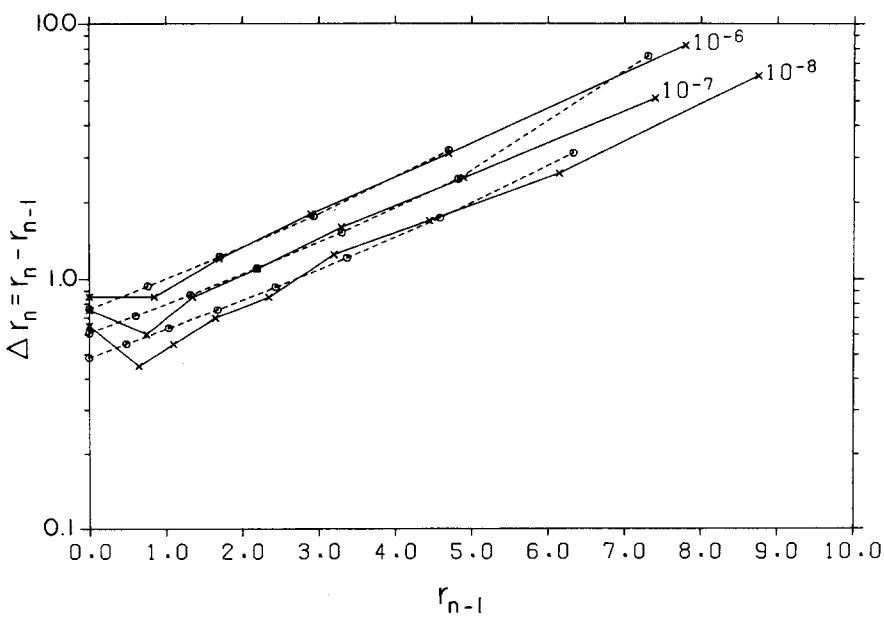

FIG. 5. Quintic "window" mesh points (solid line) for $\epsilon = 10^{-6}$, 10^{-7} and 10^{-8}, and three logarithmic meshes (broken line). The parameters for the logarithmic meshes are: $(4s+3)/2\zeta = 1/0.246$; and $A\epsilon^{1/(4s+3)} = 0.139116\times10^{1/11}$, 0.139116, $0.139116\times10^{-1/11}$. The $A\epsilon^{1/(4s+3)}$ parameter for the middle curve was chosen to place it approximately on the middle "window" curve.

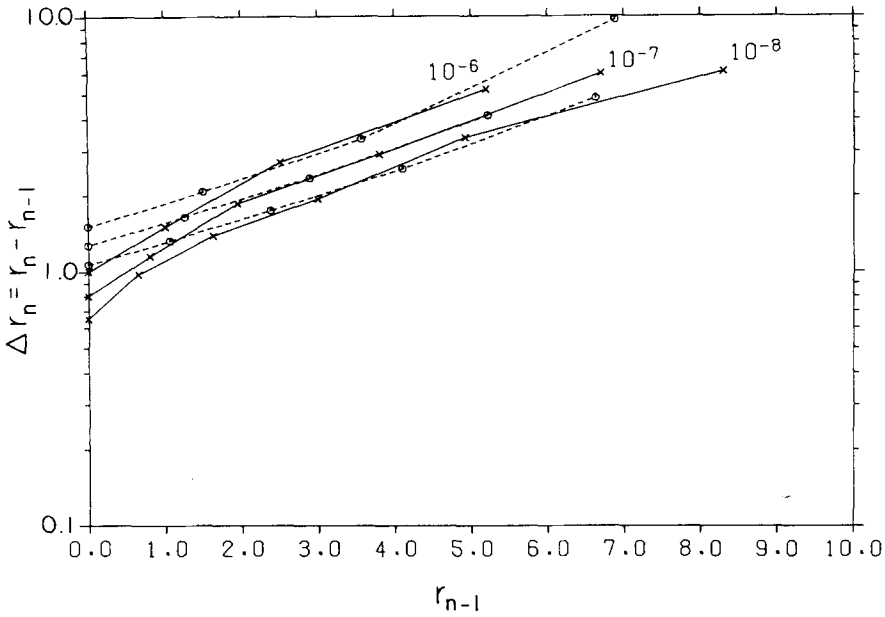

FIG. 6. Septic "window" mesh points (solid line) for $\epsilon = 10^{-6}$, 10^{-7} and 10^{-8}, and three logarithmic meshes (broken line). The parameters for the logarithmic meshes are: $(4s+3)/2\zeta = 1/0.181$; and $\Lambda\epsilon^{1/(4s+3)} = 0.203583 \times 10^{1/15}$, 0.203583, $0.203583 \times 10^{-1/15}$. The $\Lambda\epsilon^{1/(4s+3)}$ parameter for the middle curve was chosen to place it approximately on the middle "window" curve.

successive points. Especially for some of the quintic and septic calculations reported below, the relative change in $\Delta n/\Delta r$ is appreciable.

V. CALCULATIONS

A. Formulation

To illustrate the theoretical considerations of the preceding sections we have carried out variational calculations of the Hartree–Fock energy of helium by both the HIF method and the spline method, for cubic, quintic, and septic polynomials. In this subsection we explain how the calculations were set up.

Through the Hermite interpolation formula, the expectation value of any one-electron operator with respect to a piecewise polynomial function of order $2s+1$ can be expressed as

$$F = \sum_{i=0}^{s}\sum_{i'=0}^{s}\sum_{\substack{n=0\\(|n-n'|\le 1)}}^{N}\sum_{n'=0}^{N} y_n^{(i)} F_{in,i'n'} y_{n'}^{(i')} \quad . \tag{19}$$

The matrix elements $F_{in,i'n'}$ involve factors from the Hermite formula, and primitive integrals of the form

$$\int_{r_{n-1}}^{r_n} dr\, r^2 (r - r_{n-1})^j (r_n - r)^k F (r - r_{n-1})^l (r_n - r)^m \quad , \tag{20}$$

whose evaluation is straightforward and is discussed in Appendix B.

To carry out a Hartree–Fock calculation by the HIF method, one first constructs the Fock and overlap matrices. Then the eigenvalues of the Fock matrix are obtained by standard matrix methods. Each eigenvector contains a set of $y_n^{(i)}$, $(i = 0, 1, \ldots, s;\ n = 0, 1, \ldots, N)$.

Since the Fock matrix depends on the wavefunction, it is necessary to iterate to self consistency.

To carry out a Hartree–Fock calculation by the spline method one substitutes Eq. (6) into Eq. (19) to obtain the expectation value expression,

$$\langle F \rangle = \sum_{n=0}^{N}\sum_{n'=0}^{N} y_n^{(0)} \Bigg(\sum_{\substack{i,i'\\m,m'}} Z_{mn}^{(i)} F_{im,i'm'} Z_{m'n'}^{(i')} \Bigg) y_{n'}^{(0)} \quad . \tag{21}$$

Thus in the spline representation, the Fock and overlap matrices are obtained from the HIF matrices by transformation with the $\mathbf{Z}^{(i)}$ matrices. The spline representation matrices are then fed to a standard diagonalization program. Each eigenvector consists of a set of $y_n^{(0)}$, $(n = 0, 1, \ldots, N)$. Since the Fock matrix depends on the wavefunction, one must iterate to self-consistency.

It should be pointed out that the dimensionality of the matrix eigenvalue problem, as formulated above (see below), is $(s+1)\times(N+1)$ for the HIF method, and $N+1$ for the spline method. In the next subsection, we describe boundary conditions that reduce the dimensionality still further to $(s+1)\times N$ for the HIF method, and to N for the spline method.

B. Boundary conditions

The boundary condition of square integrability at infinity can be approximated by setting $y_N^{(0)}$ equal to zero. In practical terms, one simply drops the corresponding row and column of the matrices described in the preceding subsection, before finding eigenvalues and eigenvectors. In practice, we found it convenient to use even more drastic boundary conditions at r_N, which were easier to program, but which did not significantly alter the quality of the energy. In the HIF case, we took $y_N^{(i)} = 0$, $(i = 0, 1, 2, \ldots, s)$, thereby reducing the dimensionality of the matrix eigenvalue problem to $(s+1)\times N$. In the spline case, the corresponding conditions reduce the eigenvalue problem to N dimensions.

We explored other boundary conditions, such as to fix the logarithmic derivative at r_N to be $-\zeta = -\sqrt{-2\epsilon_{1s}}$, and then to append an exponential "tail." The increase in accuracy did not justify the increase in complexity.

TABLE IV. Approximate Hartree–Fock energies[a] and errors[b] for the helium atom with piecewise polynomial wavefunctions.

Cubic			Quintic			Septic		
N	Energy	Error	N	Energy	Error	N	Energy	Error
				Spline method				
7	−2.861329	(3.50×10^{-4})[c]	4	−2.860958	(7.21×10^{-4})[c,e]	9	−2.8616799573	(3.83×10^{-8})[k]
10	−2.8616292	(5.07×10^{-5})[c]	5	−2.861555	(1.24×10^{-4})[c,e]	13	−2.86167999408	(1.53×10^{-9})[l]
13	−2.86167253	(7.46×10^{-6})[d]	6	−2.8616583	(2.16×10^{-5})[c,e]			
20	−2.861679149	(8.46×10^{-7})[d]	8	−2.86167701	(2.98×10^{-6})[f,e]			
29	−2.8616798965	(9.90×10^{-8})[c]	8	−2.86167597	(4.02×10^{-6})[g]			
39	−2.8616799581	(3.75×10^{-8})[c]	9	−2.861679642	(3.53×10^{-7})[c,e]			
			10	−2.861679560	(4.35×10^{-7})[h]			
			12	−2.8616799436	(5.20×10^{-8})[i]			
			13	−2.8616799688	(2.68×10^{-8})[j,e]			
				Hermite interpolation function method				
10	−2.8616379	(4.20×10^{-5})[c]	5	−2.86167837	(1.62×10^{-6})[c]	5	−2.86167998832	(7.29×10^{-9})[o]
13	−2.86167461	(5.38×10^{-6})[d]	7	−2.8616799643	(3.13×10^{-8})[d]	6	−2.86167999394	(1.67×10^{-9})[p]
20	−2.861679436	(5.59×10^{-7})[d]	8	−2.8616799690	(2.66×10^{-8})[g]	7	−2.861679995319	(2.93×10^{-10})[q]
			9	−2.86167999083	(4.78×10^{-9})[c]	9	−2.8616799955996	(1.26×10^{-11})[r]
			10	−2.86167999288	(2.73×10^{-9})[m]	13	−2.86167999561206	(1.49×10^{-13})[l]
			10	−2.86167999218	(3.43×10^{-9})[h]	15	−2.86167999561221	$(\ ?\times10^{-14})$[s]
			12	−2.861679995140	(4.72×10^{-10})[n]			
			12	−2.861679995211	(4.01×10^{-10})[i]			
			19	−2.86167999560873	(3.48×10^{-12})[t]			

[a] In atomic units (27.2...eV).
[b] The errors are relative to the septic $N=15$ result: −2.86167999561221 a.u.
[c] "Window" mesh (Tables I–III) but with the last point replaced by $r_N=10$.
[d] "Window" mesh, but with the last two points replaced by $r_N=10$.
[e] The second derivative at the origin was taken as a variational parameter for these quintic spline calculations.
[f] "Window" mesh for "quintic, $\epsilon=10^{-7}$," but with an extra point at 0.5, and the last two points replaced by $r_N=10$.
[g] Mesh points given by Eq. (15) with $(4s+3)/2\zeta=1/0.246$, and with $\Lambda\epsilon^{1/(4s+3)}=0.126546$. An extra point was added at $r_N=15$.
[h] Same formula as for Note g, except that ϵ was decreased by a factor of 10. An extra point was added at $r_N=15$.
[i] Same formula as for Note g, except that ϵ was decreased by a factor of 100, and the last point at 28.5 was moved to $r_N=16$.
[j] Mesh points for $\epsilon=10^{-9}$, estimated from Fig. 2 (before the $\epsilon=10^{-9}$ set had been obtained by the "window" method). The mesh points are: 0.0, 0.3, 0.5, 0.8, 1.2, 1.6, 2.05, 2.6, 3.2, 3.9, 4.9, 6.3, 8.3, and 10.
[k] "Window" mesh for "quintic, $\epsilon=10^{-8}$," but with the last point moved from 15 to $r_N=12$.
[l] Mesh points given by Eq. (15) with $(4s+3)/2\zeta=1/0.181$, and with $\Lambda\epsilon^{1/(4s+3)}=0.1\times10^{-2/15}$. (Cf. Notes r and s.)
[m] "Window" mesh for "quintic, $\epsilon=10^{-8}$," but with an extra point at 10, and with the last point moved from 15 to $r_N=12$.
[n] "Window" mesh.
[o] Mesh points given by Eq. (15) with $(4s+3)/2\zeta=1/0.181$, and the $\Lambda\epsilon^{1/(4s+3)}=0.181$, the latter having been chosen to put the last point at $r_N=13$.
[p] "Window" mesh, but with the last point moved from 14.4 to $r_N=12$.
[q] Mesh points given by Eq. (15) with $(4s+3)/2\zeta=1/0.181$, and with $\Lambda\epsilon^{1/(4s+3)}=0.134805$, the latter having been chosen to put r_1 at 0.8.
[r] Mesh points given by Eq. (15) with $(4s+3)/2\zeta=1/0.181$, and with $\Lambda\epsilon^{1/(4s+3)}=0.10055$, the latter having been chosen to put the last point at $r_N=13$.
[s] Mesh points given by Eq. (15) with $(4s+3)/2\zeta=1/0.181$, and with $\Lambda\epsilon^{1/(4s+3)}=0.1\times10^{-3/15}$.
[t] Mesh points given by Eq. (15) with $(4s+3)/2=1/0.246$, and with $\Lambda\epsilon^{1/(4s+3)}=0.0516$, the latter having been chosen to put the last point at $r_N=16$.

For the spline case, it is convenient to introduce extra boundary or "end conditions," so as to be able to solve for all the derivatives in terms of the functional values. Since we take $y_N^{(0)}=0$, there are only N independent functional values, $(y_0^{(0)}, y_1^{(0)}, \ldots, y_{N-1}^{(0)})$. To eliminate the $s\times(N+1)$ quantities $y_n^{(i)}$, $(i=1, 2, \ldots, s;\ n=0, 1, \ldots, N)$ we need to add $2s$ conditions to the $s\times(N-1)$ continuity conditions. After some exploratory calculations, we found the following conditions convenient: (1) The logarithmic derivative at the origin is to be $-Z$, where $Z=2$ for helium (cusp condition); (2) $y_N^{(i)}=0$, $i=0, 1, 2, \ldots, s$; effectively this reduces the number of $y_n^{(i)}$ to be solved for, to $s\times N$; (3) $y_N^{(i)}=0$, $i=s+1, s+2, \ldots, 2s-1$; these conditions, via the Hermite interpolation formula, imply relations among the $y_{N-1}^{(i)}$, $(i\leq s)$. The implementation of these boundary conditions is discussed in Appendix A.

In the higher order spline case ($s>1$), we explored imposing fewer boundary conditions, and instead keeping the higher derivatives at the origin as variational parameters (some of these calculations are reported in Table IV). The increase in accuracy was, in our opinion, insufficient to justify the increase in complexity.

C. Computations

To demonstrate how the accuracy of the energy depends on mesh and on method, both HIF and spline calculations of the Hartree–Fock energy of helium were carried out in double precision (on a DECsystem-10

computer). Mesh points were chosen by the "window" method and by the logarithmic formula (15). In general, the accuracy was not a strong function of the position of the last point, r_N, and in the course of carrying out the calculations, we took some liberty with its location. These changes are indicated in the notes to Table IV. The energies so obtained are listed in Tables IV and V. A "log–log" plot of δE vs N, the calculated minus exact Hartree–Fock energy vs the number of points minus one, is exhibited in Fig. 7.

D. Discussion

Several points can be made immediately from Fig. 7:

(1) The $(\delta E, N)$ points fall into families, according to polynomial order $(2s+1)$ and method (spline or HIF).

(2) The locus of points for a given family is approximately a straight line.

(3) The slope of the septic lines is steeper than for the quintics, which in turn are steeper than for the cubics. The slopes are approximately given by the theoretical values, $-4s-2$, with better agreement for cubics and quintics than septics. Note again, the higher the order, the more rapid the convergence.

(4) For a given method and number of points, the "window" points and the logarithmic formula (15) usually give comparable values for the energy.

(5) For $N \sim 10$, the cubic HIF energy is not significantly lower than the cubic spline energy, but the quintic HIF energy error is 2 orders of magnitude better than the quintic spline energy error, and the septic HIF energy is more than 3 orders of magnitude more accurate than the septic spline energy. At $N \sim 10$, the overall gain in accuracy from cubics to septic HIF is approximately 7 orders of magnitude, and the difference increases rapidly as N increases.

Our experience indicates that the higher order HIF methods are more efficient in computer time than lower order HIF methods and than spline methods, for constant δE.

The lowest value we report for the Hartree–Fock energy for helium is -2.8616799956122 a.u., from an $N=15$ septic HIF calculation whose accuracy should be better than 10^{-13} a.u. The most accurate value already in the literature is -2.861679995615 a.u., obtained by Raffenetti[6] with a 12-term even tempered Slater orbital basis on IBM 360 equipment. For a more significant comparison, we recomputed Raffenetti's result to 15 decimal digits. Dr. Raffenetti kindly provided us with values of his "α" and "β" parameters to 12 significant figures (Ref. 6 reports only six) and a copy of his computer program, which was adapted to the Johns Hopkins DECsystem-10 computer by Mr. Dennis P. Carroll, Raffenetti's program on our machine gave a value that agreed with ours to less than 10^{-14} a.u. The value above, in which the last digit "2" represents 2×10^{-13} a.u., is thus obtained identically by both methods.

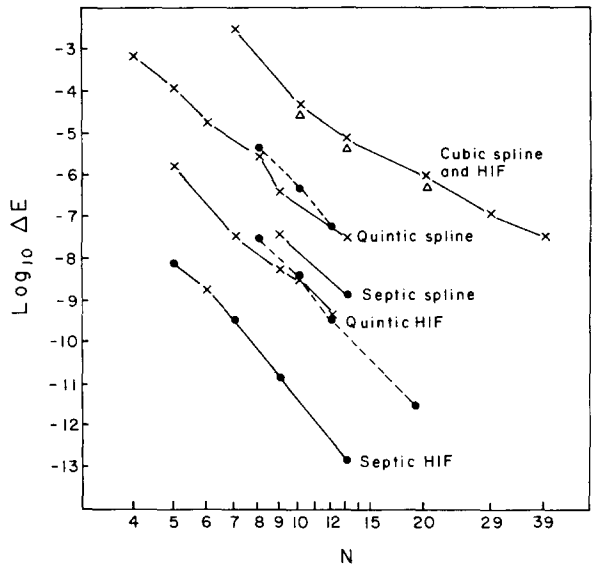

FIG. 7. LogΔE vs log$N$ for various spline and HIF calculations. The helium Hartree–Fock energy shift is relative to the $N=15$ HIF value, -2.86167999561221 a.u. Legend: ×–"Window" mesh; • –Mesh points given by logarithmic formula [Eq. (15)]; Δ–"Window" mesh, cubic HIF method.

TABLE V. Accuracy as a function of polynomial order and of method (Hermite interpolation function vs spline) for the same fixed mesh points.[a]

Method	Polynomial order	Energy (a.u.)	Error (a.u.)[b]
Spline	Cubic	−2.860628	$1.05\ 10^{-3}$
HIF	Cubic	−2.861546	$1.33\ 10^{-4}$
Spline	Qunitic	−2.861679592	$4.03\ 10^{-7}$
Spline	Septic	−2.8616799573	$3.83\ 10^{-8}$
HIF	Qunitic	−2.86167999282	$2.79\ 10^{-9}$
HIF	Septic	−2.8616799955584	$5.38\ 10^{-11}$

[a]Ten point ($N=9$) mesh, the "qunitic, $\epsilon=10^{-8}$" set from Table II, but with the last point moved from 15 to $r_N=12$.
[b]Relative to the $N=15$ septic HIF result, -2.8616799956122 a.u.

As an indication of the quality of piecewise polynomial wavefunctions, we report the cusp ratios $(2+y_0^{(1)}/y_0^{(0)} = -1.9\ 10^{-5})$ and the virial, in the form $2-V/E=-2.9\ 10^{-12}$, for the $N=15$ septic HIF polynomial wavefunction.

In the course of carrying out our computations, we noticed several numerical "phenomena":

(1) In the Hartree–Fock calculations, the orbital energy converged by 1 order of magnitude for each two iterations.

(2) The higher order spline methods tended to be numerically sensitive in unexpected ways. For instance, if we tried to set the second derivative at the origin to a slightly nonoptimum value, the quintic spline function changed drastically for all values of r.

(3) The spline methods worked better if the last interval, $r_N - r_{N-1}$, was not too large.

(4) We detected no sensitivities, convergence difficulties, or linear dependence problems in any of the HIF calculations.

VI. SUMMARY AND CONCLUSIONS

The use of piecewise polynomial electronic wavefunctions has been studied theoretically and computationally. The Hermite interpolation function method, based on Hermite's generalization of Lagrange's interpolation formula, gives generally more accurate results than the spline method, and higher order polynomials converge orders of magnitude faster than lower order, approximately according to the law (for appropriate meshes),

$$\delta E \sim N^{-(\text{polynomial order})\times 2} ,$$

where $N+1$ is the number of mesh points. No numerical instabilities with the HIF method were encountered in the course of the study, and the method appears capable of being pushed to very high accuracy in a systematic way.

ACKNOWLEDGMENT

We wish to thank Mr. Dennis P. Carroll, Mr. Randall Diffenderfer, and Dr. Richard C. Raffenetti for technical assistance, and The Johns Hopkins University for its support of the computer calculations.

APPENDIX A. THE SPLINE METHOD

We outline here the working equations of the spline method, the end result of which are the matrices $\mathbf{Z}^{(i)}$ referred to in Eq. (6).

Cubic splines

In the case of cubic splines, the i of Eq. (5) takes on only the value 2, and the continuity equations for the second derivative explicitly are

$$3(\Delta r_n)^{-2}y_{n-1}^{(0)} + 3[-(\Delta r_n)^{-2} + (\Delta r_{n+1})^{-2}]y_n^{(0)} - 3(\Delta r_{n+1})^{-2}y_{n+1}^{(0)} + (\Delta r_n)^{-1}y_{n-1}^{(1)} + 2[(\Delta r_n)^{-1} + (\Delta r_{n+1})^{-1}]y_n^{(1)} + (\Delta r_{n+1})^{-1}y_{n+1}^{(1)} = 0 , \quad (n=1, 2, \ldots, N-1) . \tag{A1}$$

Here we have used

$$\Delta r_n = r_n - r_{n-1} . \tag{A2}$$

These have the form of a matrix equation

$$\mathbf{A}^{(0)} \cdot \mathbf{y}^{(0)} + \mathbf{A}^{(1)} \cdot \mathbf{y}^{(1)} = 0 , \tag{A3}$$

where $\mathbf{y}^{(0)}$ and $\mathbf{y}^{(1)}$ are column vectors of the functional values and first derivatives, respectively, at $r=0, r_1, \ldots, r_N$. The nonzero matrix elements of $\mathbf{A}^{(0)}$ and $\mathbf{A}^{(1)}$ are $A_{n,n}^{(i)}$ and $A_{n,n\pm1}^{(i)}$, which are given by

$$A_{n,n-1}^{(0)} = 3(\Delta r_n)^{-2} , \tag{A4}$$

$$A_{n,n}^{(0)} = 3[-(\Delta r_n)^{-2} + (\Delta r_{n+1})^{-2}] , \tag{A5}$$

$$A_{n,n+1}^{(1)} = (\Delta r_{n+1})^{-1} . \tag{A6}$$

The cusp at the origin is taken care of by

$$A_{00}^{(1)} = 1 , \tag{A7}$$

$$A_{0k}^{(1)} = 0 , \quad k \neq 0 , \tag{A8}$$

$$A_{00}^{(0)} = -Z , \tag{A9}$$

$$A_{0k}^{(0)} = 0 , \quad k \neq 0 . \tag{A10}$$

The additional boundary conditions, that $y_N^{(0)}$ and $y_N^{(1)}$ be zero, are most easily incorporated by dropping column N from $\mathbf{A}^{(0)}$ and $\mathbf{A}^{(1)}$. Thus both $\mathbf{A}^{(0)}$ and $\mathbf{A}^{(1)}$ are square $N\times N$ matrices (the indices run from 0 to $N-1$). The matrix $\mathbf{Z}^{(1)}$ of Eq. (6) is then immediately given by

$$\mathbf{Z}^{(1)} = -(\mathbf{A}^{(1)})^{-1} \cdot \mathbf{A}^{(0)} . \tag{A11}$$

Quintic splines

The i in Eq. (5) takes on the values 3 and 4 for quintic splines. The two sets of equations are

$$10(\Delta r_n)^{-3}y_{n-1}^{(0)} - 10[(\Delta r_n)^{-3} + (\Delta r_{n+1})^{-3}]y_n^{(0)} + 10(\Delta r_{n+1})^{-3}y_{n+1}^{(0)} + 4(\Delta r_n)^{-2}y_{n-1}^{(1)} + 6[(\Delta r_n)^{-2} - (\Delta r_{n+1})^{-2}]y_n^{(1)} - 4(\Delta r_{n+1})^{-2}y_{n+1}^{(1)} + \tfrac{1}{2}(\Delta r_n)^{-1}y_{n-1}^{(2)} - (\tfrac{3}{2})[(\Delta r_n)^{-1} - (\Delta r_{n+1})^{-1}]y_n^{(2)} - \tfrac{1}{2}(\Delta r_{n+1})y_{n+1}^{(2)} = 0 , \quad (n=1, 2, \ldots, N-1) ; \tag{A12}$$

$$15(\Delta r_n)^{-4}y_{n-1}^{(0)} - 15[(\Delta r_n)^{-4} - (\Delta r_{n+1})^{-4}]y_n^{(0)} - 15(\Delta r_{n+1})^{-4}y_{n+1}^{(0)} + 7(\Delta r_n)^{-3}y_{n-1}^{(1)} + 8[(\Delta r_n)^{-3} + (\Delta r_{n+1})^{-3}]y_n^{(1)} + 7(\Delta r_{n+1})^{-3}y_{n+1}^{(1)} + (\Delta r_n)^{-2}y_{n-1}^{(2)} - (\tfrac{3}{2})[(\Delta r_n)^{-2} - (\Delta r_{n+1})^{-2}]y_n^{(2)} - (\Delta r_{n+1})^{-2}y_{n+1}^{(2)} = 0 , \quad (n=1, 2, \ldots, N-1) . \tag{A13}$$

These have the form of matrix equations,

$$\mathbf{A}^{(3,0)} \cdot \mathbf{y}^{(0)} + \mathbf{A}^{(3,1)} \cdot \mathbf{y}^{(1)} + \mathbf{A}^{(3,2)} \cdot \mathbf{y}^{(2)} = 0 , \tag{A14}$$

$$\mathbf{A}^{(4,0)} \cdot \mathbf{y}^{(0)} + \mathbf{A}^{(4,1)} \cdot \mathbf{y}^{(1)} + \mathbf{A}^{(4,2)} \cdot \mathbf{y}^{(2)} = 0 , \tag{A15}$$

where the superscripts 3 and 4 refer to the value of i in Eq. (5), and where the nonzero values of $\mathbf{A}^{(i,j)}$, which are $A_{n,n}^{(i,j)}$ and $A_{n,n\pm1}^{(i,j)}$, can be read off directly from Eqs. (A9) and (A10) [cf. Eqs. (A1)–(A4)]. The cusp at the origin is taken care of by adding a row to $\mathbf{A}^{(3,0)}$, $\mathbf{A}^{(3,1)}$, and $\mathbf{A}^{(3,2)}$:

$$A_{00}^{(3,1)} = 1 , \tag{A16}$$

$$A_{0k}^{(3,1)} = 0 , \quad k \neq 0 , \tag{A17}$$

$$A_{00}^{(3,0)} = -Z , \tag{A18}$$

$$A_{0,k}^{(3,0)} = 0 , \quad k \neq 0 , \tag{A19}$$

$$A_{0,k}^{(3,2)} = 0 , \quad \text{all } k . \tag{A20}$$

The boundary conditions that $y_N^{(0)}$, $y_N^{(1)}$, $y_N^{(2)}$ be zero are incorporated by dropping column N from the $\mathbf{A}^{(i,j)}$. The additional condition that $y_N^{(3)}$ vanish is

$$10(\Delta r_n)^{-3}y_{N-1}^{(0)} + 4(\Delta r_N)^{-2}y_{N-1}^{(1)} + \tfrac{1}{2}(\Delta r_N)^{-1}y_{N-1}^{(2)} = 0 , \tag{A21}$$

which can be taken care of by adding a row to $\mathbf{A}^{(4,0)}$, $\mathbf{A}^{(4,1)}$, and $\mathbf{A}^{(4,2)}$:

$$A_{0,N-1}^{(4,0)} = 10(\Delta r_N)^{-3} , \tag{A22}$$

$$A_{0,N-1}^{(4,1)} = 4(\Delta r_N)^{-2} , \tag{A23}$$

$$A_{0,N-1}^{(4,2)} = \tfrac{1}{2}(\Delta r_N)^{-1} , \tag{A24}$$

$$A^{(4,i)}_{0,k} = 0 \ , \quad k \neq N-1 \ . \tag{A25}$$

The six $\mathbf{A}^{(i,j)}$, $(i=3, 4;\ j=0, 1, 2)$, so constructed are $N\times N$ square matrices. If we solve Eq. (A15) for $\mathbf{y}^{(2)}$ and substitute the result into Eq. (A14), we obtain

$$\mathbf{y}^{(2)} = -(\mathbf{A}^{(4,2)})^{-1} \cdot \mathbf{A}^{(4,0)} \cdot \mathbf{y}^{(0)} - (\mathbf{A}^{(4,2)})^{-1} \cdot \mathbf{A}^{(4,1)} \cdot \mathbf{y}^{(1)} , \tag{A26}$$

$$[\mathbf{A}^{(3,0)} - \mathbf{A}^{(3,2)} \cdot (\mathbf{A}^{(4,2)})^{-1} \cdot \mathbf{A}^{(4,0)}] \cdot \mathbf{y}^{(0)} + [\mathbf{A}^{(3,1)} - \mathbf{A}^{(3,2)} \cdot (\mathbf{A}^{(4,2)})^{-1} \cdot \mathbf{A}^{(4,1)}] \cdot \mathbf{y}^{(1)} = 0 \ . \tag{A27}$$

Equation (A27) has the same form as the cubic spline Eq. (A3), and can be similarly solved for $\mathbf{Z}^{(1)}$ [Eq. (A11)]. The $\mathbf{Z}^{(2)}$ can be obtained from Eq. (A26):

$$Z^{(2)} = -(\mathbf{A}^{(4,2)})^{-1} \cdot (\mathbf{A}^{(4,0)} + \mathbf{A}^{(4,1)} \cdot \mathbf{Z}^{(1)}) \ . \tag{A28}$$

Septic splines

In the case of septic splines, the i of Eq. (5) takes on the values 4, 5, and 6. The three sets of equations are

$$35(\Delta r_n)^{-4} y^{(0)}_{n-1} - 35[(\Delta r_n)^{-4} - (\Delta r_{n+1})^{-4}] y^{(0)}_n - 35 y^{(0)}_{n+1} + 15(\Delta r_n)^{-3} y^{(1)}_{n-1} + 20[(\Delta r_n)^{-3} + (\Delta r_{n+1})^{-3}] y^{(1)}_n + 15 y^{(1)}_{n+1} + (\tfrac{5}{2})(\Delta r_n)^{-2} y^{(2)}_{n-1}$$
$$- 5[(\Delta r_n)^{-2} - (\Delta r_{n+1})^{-2}] y^{(2)}_n - (\tfrac{5}{2}) y^{(2)}_{n+1} + (\tfrac{1}{6})(\Delta r_n)^{-1} y^{(3)}_{n-1} + \tfrac{2}{3}[(\Delta r_n)^{-1} + (\Delta r_{n+1})^{-1}] y^{(3)}_n + (\tfrac{1}{6}) y^{(3)}_{n+1} = 0 , \quad (n=1, 2, \ldots, N-1) , \tag{A29}$$

$$84(\Delta r_n)^{-5} y^{(0)}_{n-1} - 84[(\Delta r_n)^{-5} + (\Delta r_{n+1})^{-5}] y^{(0)}_n - 84 y^{(0)}_{n+1} + 39(\Delta r_n)^{-4} y^{(1)}_{n-1} + 45[(\Delta r_n)^{-4} - (\Delta r_{n+1})^{-4}] y^{(1)}_n - 39 y^{(1)}_{n+1} + 7(\Delta r_n)^{-3} y^{(2)}_{n-1}$$
$$- 10[(\Delta r_n)^{-3} + (\Delta r_{n+1})^{-3}] y^{(2)}_n + 7 y^{(2)}_{n+1} + \tfrac{1}{2}(\Delta r_n)^{-2} y^{(3)}_{n-1} + [(\Delta r_n)^{-2} - (\Delta r_{n+1})^{-2}] y^{(3)}_n - \tfrac{1}{2} y^{(3)}_{n+1} = 0 , \quad (n=1, 2, \ldots, N-1) , \tag{A30}$$

$$70(\Delta r_n)^{-6} y^{(0)}_{n-1} - 70[(\Delta r_n)^{-6} - (\Delta r_{n+1})^{-6}] y^{(0)}_n - 70(\Delta r_{n+1})^{-6} y^{(0)}_{n+1} + 34(\Delta r_n)^{-5} y^{(1)}_{n-1} + 36[(\Delta r_n)^{-5} + (\Delta r_{n+1})^{-5}] y^{(1)}_n + 34(\Delta r_{n+1})^{-5} y^{(1)}_{n+1}$$
$$+ (\tfrac{13}{2})(\Delta r_n)^{-4} y^{(2)}_{n-1} - (\tfrac{15}{2})[(\Delta r_n)^{-4} - (\Delta r_{n+1})^{-4}] y^{(2)}_n - (\tfrac{13}{2})(\Delta r_{n+1})^{-4} y^{(2)}_{n+1} + \tfrac{1}{2}(\Delta r_n)^{-3} y^{(3)}_{n-1} + (\tfrac{2}{3})[(\Delta r_n)^{-3} + (\Delta r_{n+1})^{-3}] y^{(3)}_n + \tfrac{1}{2}(\Delta r_{n+1})^{-3} y^{(3)}_{n+1} = 0 ,$$
$$(n=1, 2, \ldots, N-1) . \tag{A31}$$

As with the cubics and quintics, Eqs. (A29)–(A31) have the form of matrix equations,

$$\mathbf{B}^{(i,0)} \cdot \mathbf{y}^{(0)} + \mathbf{B}^{(i,1)} \cdot \mathbf{y}^{(1)} + \mathbf{B}^{(i,2)} \cdot \mathbf{y}^{(2)} + \mathbf{B}^{(i,3)} \cdot \mathbf{y}^{(3)} = 0 , \quad (i=4, 5, 6) , \tag{A32}$$

where the principal nonzero elements of the $\mathbf{B}^{(i,j)}$ can be read off from Eqs. (A29)–(A31). We put the cusp condition into the first row of the $\mathbf{B}^{(4,j)}$:

$$B^{(4,0)}_{0,0} = -Z \ , \tag{A33}$$

$$B^{(4,0)}_{0,k} = 0 \ , \quad k \neq 0 \ , \tag{A34}$$

$$B^{(4,1)}_{0,0} = 1 \ , \tag{A35}$$

$$B^{(4,1)}_{0,k} = 0 \ , \quad k \neq 0 \ , \tag{A36}$$

$$B^{(4,i)}_{0,k} = 0 \ , \quad i=2, 3, \text{ all } k \ . \tag{A37}$$

We incorporate the conditions $y^{(i)}_N = 0$, $(i=0, 1, 2, 3)$, by dropping column N from the matrices. The additional conditions that $y^{(4)}_N$ and $y^{(5)}_N$ vanish are

$$35(\Delta r_N)^{-4} y^{(0)}_{N-1} + 15(\Delta r_N)^{-3} y^{(1)}_{N-1} + (\tfrac{5}{2})(\Delta r_N)^{-2} y^{(2)}_{N-1} + (\tfrac{1}{6})(\Delta r_N)^{-1} y^{(3)}_{N-1} = 0 , \tag{A38}$$

$$84(\Delta r_N)^{-5} y^{(0)}_{N-1} + 39(\Delta r_N)^{-4} y^{(1)}_{N-1} + 7(\Delta r_N)^{-3} y^{(2)}_{N-1} + \tfrac{1}{2}(\Delta r_N)^{-2} y^{(3)}_{N-1} = 0 \ . \tag{A39}$$

These can be put into the first rows of $B^{(5,j)}$ and $B^{(6,j)}$, respectively:

$$B^{(5,0)}_{0,N-1} = 35(\Delta r_N)^{-4} , \tag{A40}$$

$$B^{(5,1)}_{0,N-1} = 15(\Delta r_N)^{-3} , \tag{A41}$$

$$B^{(5,2)}_{0,N-1} = (\tfrac{5}{2})(\Delta r_N)^{-2} , \tag{A42}$$

$$B^{(5,3)}_{0,N-1} = (\tfrac{1}{6})(\Delta r_N)^{-1} , \tag{A43}$$

$$B^{(5,j)}_{0,k} = 0 \ , \quad k \neq N-1 , \tag{A44}$$

$$B^{(6,0)}_{0,N-1} = 84(\Delta r_N)^{-5} , \tag{A45}$$

$$B^{(6,1)}_{0,N-1} = 39(\Delta r_N)^{-4} , \tag{A46}$$

$$B^{(6,2)}_{0,N-1} = 7(\Delta r_N)^{-3} , \tag{A47}$$

$$B^{(6,3)}_{0,N-1} = \tfrac{1}{2}(\Delta r_N)^{-2} , \tag{A48}$$

$$B^{(6,j)}_{0,k} = 0 \ , \quad k \neq N-1 \ . \tag{A49}$$

The nine $\mathbf{B}^{(i,j)}$ so constructed are square $N\times N$ matrices. If we solve Eq. (A32), with $i=6$, for $\mathbf{y}^{(3)}$, and then substitute in the two matrix equations (A32) for $i=4$ and 5, we obtain

$$\mathbf{y}^{(3)} = -(\mathbf{B}^{(6,3)})^{-1}[\mathbf{B}^{(6,0)} \cdot \mathbf{y}^{(0)} + \mathbf{B}^{(6,1)} \cdot \mathbf{y}^{(1)} + \mathbf{B}^{(6,2)} \cdot \mathbf{y}^{(2)}] , \tag{A50}$$

$$\sum_{j=0}^{2} [\mathbf{B}^{(i,j)} - \mathbf{B}^{(i,3)} \cdot (\mathbf{B}^{(6,3)})^{-1} \cdot \mathbf{B}^{(6,j)}] \cdot \mathbf{y}^{(j)} = 0 , \quad (i=4, 5) \ . \tag{A51}$$

But Eqs. (A50) and (A51) are formally identical to the quintic spline case, which we just solved.

APPENDIX B

The quantum mechanical integrals that arise with polynomial wavefunctions are so simple, that they hardly seem to merit comment. Nevertheless, there is a subtlety that can lead to difficulties: the easiest analytical route—to express all integrals as sums of integrals of monomials, r^k—can be plagued by the kind of cancellation error typified by the exponential catastrophe discussed in Sec. II. To avoid the worst of such problems, it is wise to keep intact the factors

$$(r - r_{n-1})^i (r_n - r)^j (r_n - r_{n-1})^{-i-j} \tag{B1}$$

that appear in the Hermite interpolation formula. As an aid to the interested reader, we sketch the evaluation of integrals over such basis functions.

The primitive integral, to which terms all the others can be reduced, is

$$(i,j)^{(n)} = \int_{r_{n-1}}^{r_n} dr (r-r_{n-1})^i (r_n-r)^j (r_n-r_{n-1})^{-i-j} \tag{B2}$$

$$= (r_n-r_{n-1}) i!\,j!/(i+j+1)! \tag{B3}$$

$$= (r_n-r_{n-1}) B(i+1,j+1) \tag{B4}$$

$$= (r_n-r_{n-1})(i+j+1)^{-1} \Big/ \binom{i+j}{i} . \tag{B5}$$

The $B(n,m)$ is the "beta function."

The primitive "nuclear attraction integral" can be expressed in terms of the $(i,j)^{(n)}$ by

$$V_{ij}^{(n)} \equiv \int_{r_{n-1}}^{r_n} dr\, r \frac{(r-r_{n-1})^i (r_n-r)^j}{(r_n-r_{n-1})^{i+j}} \tag{B6}$$

$$= r_{n-1}(i,j)^{(n)} + (r_n-r_{n-1})(i+1,j)^{(n)} . \tag{B7}$$

The primitive "overlap integral" is easily expressed in terms of the V integrals:

$$S_{ij}^{(n)} \equiv \int_{r_{n-1}}^{r_n} dr\, r^2 \frac{(r-r_{n-1})^i (r_n-r)^j}{(r_n-r_{n-1})^{i+j}} \tag{B8}$$

$$= r_{n-1} V_{ij}^{(n)} + (r_n-r_{n-1}) V_{i+1,j}^{(n)} . \tag{B9}$$

The primitive "kinetic energy integral" is a bit more involved. One formula is

$$T_{ij,kl}^{(n)} \equiv \frac{1}{2} \int_{r_{n-1}}^{r_n} dr \frac{(d/dr) r (r-r_{n-1})^i (r_n-r)^j}{(r_n-r_{n-1})^{i+j}} \frac{(d/dr) r (r-r_{n-1})^k (r_n-r)^l}{(r_n-r_{n-1})^{k+l}} , \tag{B10}$$

$$\begin{aligned} &= (r_n-r_{n-1})^2 (1+i+j)(1+k+l)(i+k,j+l)^{(n)} + (r_n-r_{n-1}) r_{n-1} [k(1+i+j)+i(1+k+l)](i+k-1,j+l)^{(n)} \\ &\quad - (r_n-r_{n-1}) r_n [l(1+i+j)+j(1+k+l)](i+k,j+l-1)^{(n)} + r_{n-1}^2 ik (i+k-2,j+l)^{(n)} \\ &\quad + r_n^2 jl (i+k,j+l-2)^{(n)} - r_{n-1} r_n (il+jk)(i+k-1,j+l-1)^{(n)} . \end{aligned} \tag{B11}$$

The primitive "Coulomb integral" can have two electrons interacting on different subintervals or on the same subinterval. For different subintervals, the formula reflects an elementary electrostatic result:

$$C_{ij,kl}^{(n,m)} \equiv \int_{r_{n-1}}^{r_n} dr\, r^2 \int_{r_{m-1}}^{r_m} dr'\, r'^2 \frac{(r-r_{n-1})^i (r_n-r)^j}{(r_n-r_{n-1})^{i+j}} \frac{1}{r_>} \frac{(r'-r_{m-1})^k (r_m-r')^l}{(r_m-r_{m-1})^{k+l}} \tag{B12}$$

$$= V_{ij}^{(n)} S_{kl}^{(m)} , \quad (n>m) . \tag{B13}$$

For r and r_n' on the same subinterval, we give only one of several equivalent formulas:

$$\begin{aligned} C_{ij,kl}^{(n,n)} &= (r_n-r_{n-1}) \sum_{t=0}^{l} \Big\{ r_{n-1}^2 \binom{l}{t} B(k+1,t+1) V_{i+k+t+1,j+l-t}^{(n)} \\ &\quad + 2 r_{n-1} (r_n-r_{n-1}) \binom{l}{t} B(k+2,t+1) V_{i+k+t+2,j+l-t}^{(n)} + (r_n-r_{n-1})^2 \binom{l}{t} B(k+3,t+1) V_{i+k+t+3,j+l-t}^{(n)} \Big\} \\ &\quad + \sum_{t=0}^{k} r_{n-1} (r_n-r_{n-1}) \binom{k}{t} B(l+1,t+1) S_{i+k-t,j+l+t+1}^{(n)} + \sum_{t=0}^{k+1} (r_n-r_{n-1})^2 \binom{k+1}{t} B(l+1,t+1) S_{i+k-t+1,j+l+t+1}^{(n)} . \end{aligned} \tag{B14}$$

*Supported in part by the Facultad de Quimica, Universidad Nacional Autónoma de México–Banco de México.

† Present address: Facultad de Química, Universidad Nacional Autónoma de México, Cd. Universitaria, México 20 D. F., México.

[1] B. W. Shore, J. Chem. Phys. **58**, 3855 (1973).
[2] B. W. Shore, J. Phys. B **6**, 1923 (1973).
[3] B. W. Shore, J. Chem. Phys. **63**, 3835 (1975).
[4] T. L. Gilbert and P. J. Bertoncini, J. Chem. Phys. **61**, 3026 (1974).
[5] A. Altenberger-Siczek and T. L. Gilbert, J. Chem. Phys. **64**, 432 (1976).
[6] R. C. Raffenetti, J. Chem. Phys. **59**, 5936 (1973).
[7] Ch. Hermite, J. reine angew. Math. **84**, 70 (1878).
[8] See, for instance, Martin H. Schultz, *Spline Analysis* (Prentice-Hall, Englewood Cliffs, 1973). Schultz discusses the application of the spline method to eigenvalue problems.